Available online at www.sciencedirect.com
ScienceDirect
Journal of the European Ceramic Society 31 (2011) 1155–1164
www.elsevier.com/locate/jeurceramsoc

Original Article

Oxidation resistance of highly porous CVD-SiC coated Tyranno fiber composites

N. Cocera, N. Remirez de Esparza, I. Ocaña, J.M. Sanchez *

CEIT and TECNUN, Paseo Manuel de Lardizábal 15, 20018, San Sebastián, Gipuzkoa, Basque Country, Spain

Received 4 October 2010; received in revised form 7 December 2010; accepted 17 December 2010
Available online 15 January 2011

Abstract

Oxidation tests have been carried out on highly porous ceramic matrix fiber composites consisting of Tyranno Lox M fibers coated with Pyro C and CVD-SiC thin layers. TGA experiments carried out at 900 °C confirm that mass loss rates are higher for materials with thicker Pyro C layers. At higher temperatures (i.e. 1250 °C) such differences are not significant likely due to the interaction between SiC oxidation and Pyro C burnout. These tests clearly show that the oxidation kinetics of Tyranno fibers are much faster than those of CVD-SiC coatings. Therefore, the CVD-SiC coatings protect the Tyranno fibers against oxidation, although this is less effective as the thickness of the Pyro C layer increases. Finally, it has been found that the oxidation kinetics of the CVD-SiC layers are faster as the coating thickness increases and are different for the inner and the outer coating surfaces.

Keywords: Silicon carbide; Tyranno fibers; CVD-SiC; Porous composites; Oxidation resistance

1. Introduction

Silicon carbide fiber based ceramic matrix composites (CMCs) are commonly used in a wide variety of high temperature structural applications due their excellent combination of mechanical and chemical properties (i.e. strength retention above 1200 °C, resistance to thermal shock, good oxidation and corrosion behavior, etc.).[1–4] These composites are typically based on Si–C–O or Si–Ti–C–O fibers (corresponding to Nicalon® and Tyranno® commercial names respectively) and SiC matrices obtained by chemical vapor deposition (CVD) from several organometallic compounds.[5] With regard to the fibers, the two mentioned groups present similar microstructures mainly consisting of β-SiC nanocrystals and free carbon embedded in an amorphous silicon oxycarbide matrix (SiC_xO_y).[6] In general, the fiber oxidation rates depend on the selected temperature range. Thus, below 1200 °C for the Si–C–O system and 1350 °C for Si–Ti–C–O fibers, oxidation kinetics are typically parabolic and not strongly affected by their free carbon and oxycarbide contents, with activation energies ranging from 70 to 110 kJ/mol.[4,7,8] Above these temperatures, oxidation kinetics are much faster likely due to the decomposition of the oxycarbide phases, which occurs at the abovementioned temperatures with emission of CO and SiO gases.[9,10] It is believed that the pressure induced by these gases at the fiber/oxide interface is enough to break the outer silica layer allowing a direct access of oxygen to the unoxidized part of the fiber.[11–13] For highly pure CVD-SiC materials, oxidation kinetics are found to be parabolic up to much higher temperatures (i.e. 1675 °C).[14–19] Below 1400 °C, it is believed that the controlling step is the inward diffusion of O_2 through the silica scale. However, at higher temperatures, measurements carried out with the isotope exchange technique suggest a transition from molecular oxygen to network atomic oxygen diffusion.[20–22] These phenomena are still not well understood since diffusion is affected by the crystallization of the silica layer to crystoballite and the corresponding diffusivity coefficients of oxygen species in this phase are still unknown.[4,14] In addition, there is also no explanation for the differences found in the oxidation rates of pure SiC single crystals as a function of their crystallographic orientation leading to significant differences in the corresponding activation energies (from 94 kJ/mol for the $(0\,0\,0\,\bar{1})$ face to 285 kJ/mol for the (0 0 0 1) face). On the other hand, most of the works related to oxidation of SiC-C-SiC CMCs (specifically SiC/Pyro-C/CVD-SiC materials) are

* Corresponding author. Tel.: +34 943 212800; fax: +34 943 213076.
E-mail address: jmsanchez@ceit.es (J.M. Sanchez).

0955-2219/$ – see front matter © 2010 Elsevier Ltd. All rights reserved.
doi:10.1016/j.jeurceramsoc.2010.12.024

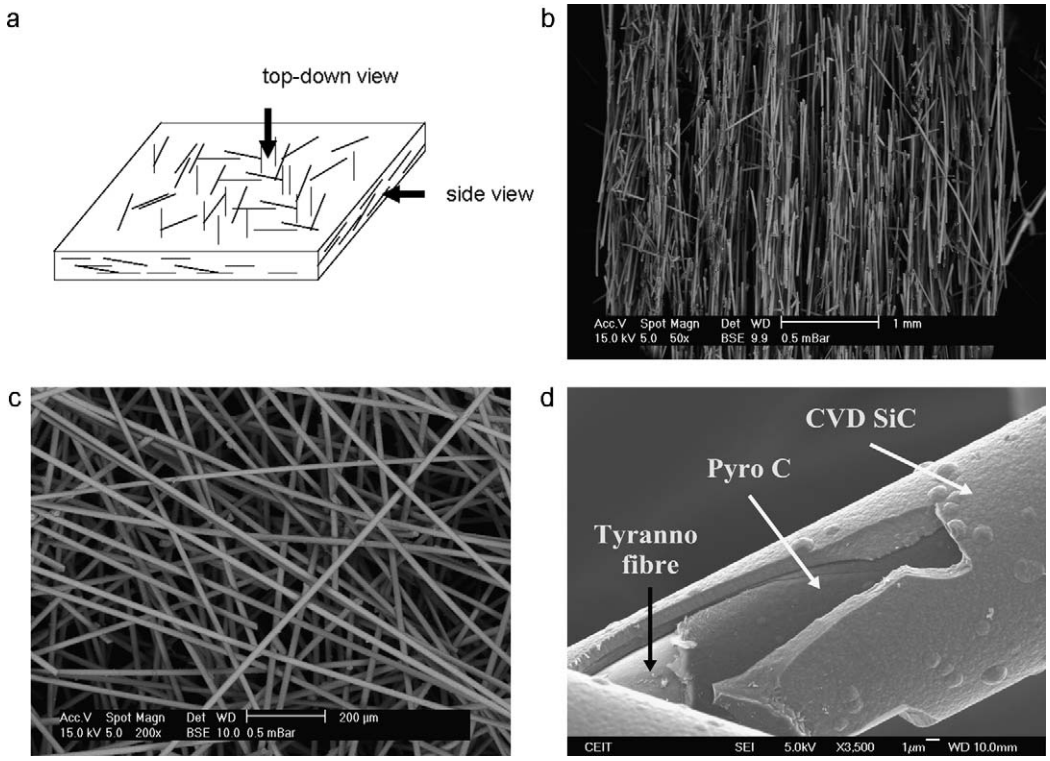

Fig. 1. (a) Scheme of the structure of the porous Tyranno/Pyro C/CVD-SiC composites, (b) BSE-SEM image of the composite side view, (c) Id. top down view and (d) detail of a broken fiber showing the three different constituents of the composite: Lox M Tyranno fiber, Pyro C layer and- CVD-SiC coating.

focused on compositions used for the fabrication of high temperature load bearing components.[1,5,23] In this case, oxidation resistance is typically studied in relation with the deterioration of the CMC mechanical properties. When a SiC/C/SiC composite is exposed to an oxidizing atmosphere, the carbon interface is the first constituent to react (starting around 450 °C) leading to CO and CO_2 emissions.[24] As a result of this reaction, the C interface disappears leaving an annular pore around each fiber. As the oxygen diffuses along these pores, it also reacts with their walls forming silica layers both at the fiber surface at the inner CVD-SiC surface. At high temperatures (above 1100 °C) and for thin carbon interfaces, the pore resulting from its gasification is closed once the growing silica layers get in contact. Therefore, oxidation is limited to a thin region near the CMC outer surface. On the other hand, at low temperatures (600–700 °C) the growth kinetics of the silica layers are extremely low and the oxidation progresses through the whole thickness of the component. Recently, a new family of highly porous SiC/Pyro C/CVD-SiC CMC composites has been developed for their application not as a structural materials but as thermal insulators or heat resistant noise absorbers[25,26] (Fig. 1). These materials are processed in two steps. Firstly, the fibers are dispersed into an aqueous medium containing a certain amount of polymer additions. Once the mixture is homogeneous, the fibers are flocculated and the water removed in order to obtain a thin laminated preform.[27,28] These preforms, in which fibers are only slightly bonded by PVA filaments, present porosity levels higher than 95 vol.%. In a second step, the fibers are more strongly bonded by a SiC film deposited by CVD. As described above, many works have been published on the oxidation resistance of dense SiC/Pyro C/CVD-SiC CMCs. However, no oxidation data are available for high porosity materials like those selected in this investigation. Under these premises, this work is aimed at analyzing the oxidation phenomena occurring in these new type of CMCs, specially the relationship between the oxidation kinetics of the three main constituents (i.e. Tyranno fibers, pyrolytic C and the CVD-SiC coating) and the overall composite oxidation behavior.

2. Experimental procedure

Preforms were obtained by dispersing the Lox M Tyranno fibers into water based solution containing 5% of polyvinyl alcohol (PVA). Once the mixture is homogeneous, the water is removed obtaining laminates of controlled thickness. Although the Tyranno fibers present a certain degree of orientation in the lamination direction (side view in Fig. 1a and b), from a top down view, they appear oriented at random (Fig. 1c). Preforms are consolidated following a process similar to that used for the fabrication dense SiC/C/SiC CMCs consisting on the subsequent deposition of Pyro C and SiC layers (Fig. 1d) (see Ref.[5] for a detailed description). The thickness of these layers is much lower than that required in dense products, since only a few microns are needed to hold together the porous fiber structure. Propane and methyltrichlorosilane (MTS) were the initial gaseous reactant species and different processing conditions were applied in order to modify the thickness of the abovementioned layers (Fig. 2). This is also reflected in the general chemical composition of the processed materials, given in Table 1, since the PyC thickness is proportional to the free C content (after subtracting the mass corresponding to the CVD SiC layer, which is different in each

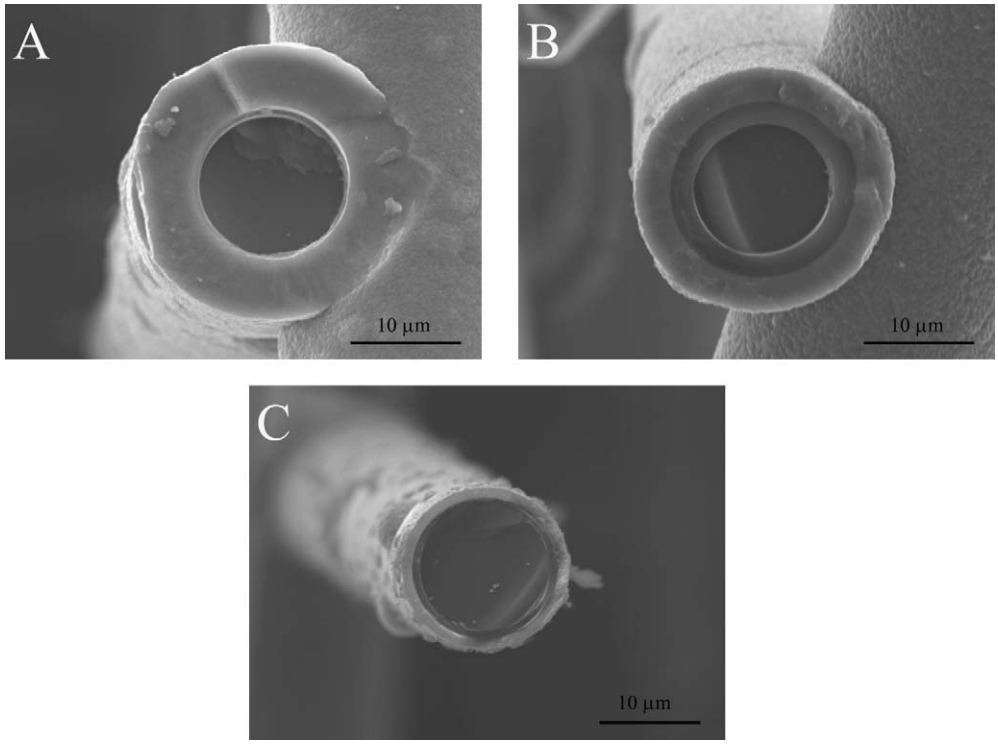

Fig. 2. FEG-SEM images of the three selected Tyranno/Pyro C/CVD SiC composites showing the different thicknesses of the Pyro C and CVD-SiC layers.

Table 1
Chemical composition of the processed SiC/pyro C/CVD-SiC fiber composites.

Reference	Chemical composition (at.%)				
	Si	C	O	Ti	% free C
A	36.97	57.46	5.25	0.32	20.49
B	35.93	60.76	3.11	0.19	24.83
C	31.69	60.14	7.70	0.47	28.45

case). Porosity values were calculated by means of picnometry experiments and geometrical measurements of the CVD coated laminates (Table 2). In all cases, porosity volume fractions were between 96 and 97 vol.%. The diameters of as-received Tyranno fibers and the thickness of Pyro C and CVD SiC layers were obtained from SEM images of samples mounted on epoxy resin and polished down to 1 μm diamond paste (Fig. 3). A set of 50 different fibers were measured for each material.

These measurements show that Lox M Tyranno fibers present an average diameter of 13.6 μm with a very narrow dispersion (95%C.I. = 0.1 μm). These data also show that the thickness of the Pyro C layer is similar for materials A and C (0.99 ± 0.03 μm and 0.92 ± 0.03 μm respectively) and higher for material B (2.20 ± 0.07 μm). On the other hand, the thickness of the CVD-SiC coating is similar for materials A and B (between 2.5 and 4.5 μm) and much lower for material C (0.82 ± 0.04 μm). The surface area of the composites was measured by the BET method using nitrogen as the adsorbing gas (ISO 9277:1995).

Table 2
Density and porosity values corresponding to the different compositions.

Reference	Actual density (g/cm^3)	Geometrical density (g/cm^3)	Porosity (%)
A	0.10	2.74	96.3
B	0.08	2.28	96.4
C	0.07	2.52	97.1

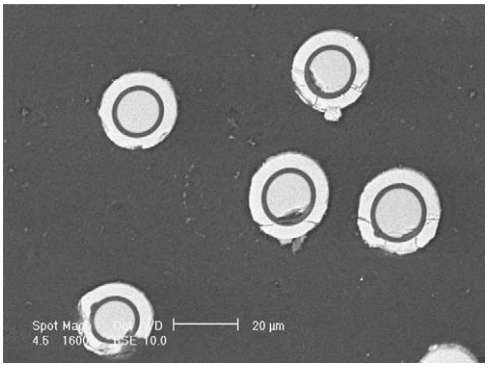

Fig. 3. BSE-SEM image corresponding to a polished sample of material "B" used for the measurement of the Tyranno fiber diameters an the thickness of Pyro C and CVD-SiC layers.

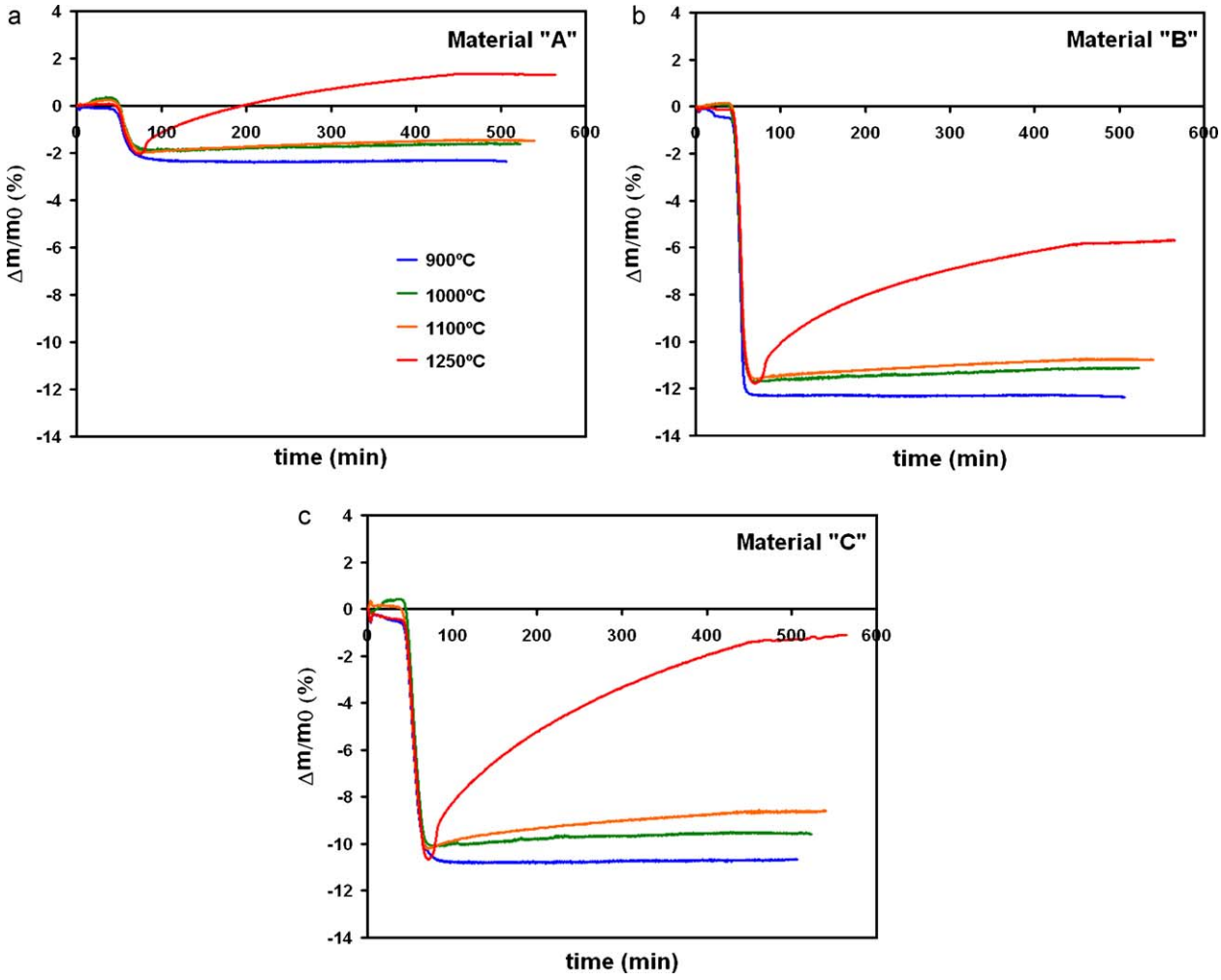

Fig. 4. TGA curves corresponding to the three different Tyranno/Pyro C/CVD SiC composites. The thermal cycles were carried out at temperatures ranging from 900 °C to 1250 °C in synthetic air ($pO_2 = 0.25$ atm) with a dwelling time of 6 h and a constant heating rate of 15 °C/min.

Oxidation kinetics were analyzed by means of high resolution thermogravimetry (TGA) on samples with an initial mass of 15 mg (sensitivity: 0.01 mg). The thermal cycles were carried out at temperatures ranging from 900 °C to 1250 °C in synthetic air ($pO_2 = 0.25$ atm) with a dwelling time of 6 h and a constant heating rate of 15 °C/min. Additional tests were carried out in industrial muffles at the same temperatures and heating rate but for a longer dwelling time; 100 h. Finally, the long term oxidation behavior was studied in samples oxidized at 1100 °C for 2000 h. Samples of 50 mm × 50 mm × 3 mm were used in these two types of experiments. As described for the starting materials, SEM images of polished samples were used for measuring the thickness of the oxide layers produced by the different thermal treatments. Mean values and 95% confidence intervals were obtained from a total number of 50 fibers measured for each material and condition.

3. Results and discussion

Thermogravimetric curves present similar characteristics for the three investigated materials (Fig. 4). Firstly, significant mass losses are detected during the heating ramp and the initial part of the temperature "plateau". Afterwards, mass losses are reduced reaching a minimum whose position depends on the temperature and the material composition. From this point on, the mass increases at a rate which is higher as the temperature increases.

First mass losses are associated to the oxidation of the Pyro C layers. According to the literature, this phenomenon starts at 450 °C with different kinetics depending on the access of oxygen to the Pyro C coating.[5] This is consistent with the values of the minimums observed in the derivatives of TGA curves (corresponding to the maximum mass loss rates) (Fig. 5a and c). Thus, the highest mass loss rate (4×10^{-3} s^{-1}) was measured for the material with the thickest Pyro C layer (i.e. composite "B") at 640–650 °C and the lowest (6.5×10^{-4} s^{-1}) was measured for the material with the thinnest Pyro C layer (composite "A") at 715–720 °C.

According to Ref.[5], above 750 °C both the Tyranno fibers and the CVD-SiC coatings start to oxidize leading to relative mass gains. The interaction between these processes and the Pyro C burnout explains the minimums observed in TGA curves. As shown in Fig. 5b and d, the position of the minimums (defined by the intersection of the TGA derivatives with the *x* axis) changes with the temperature and the material composition. Thus, for

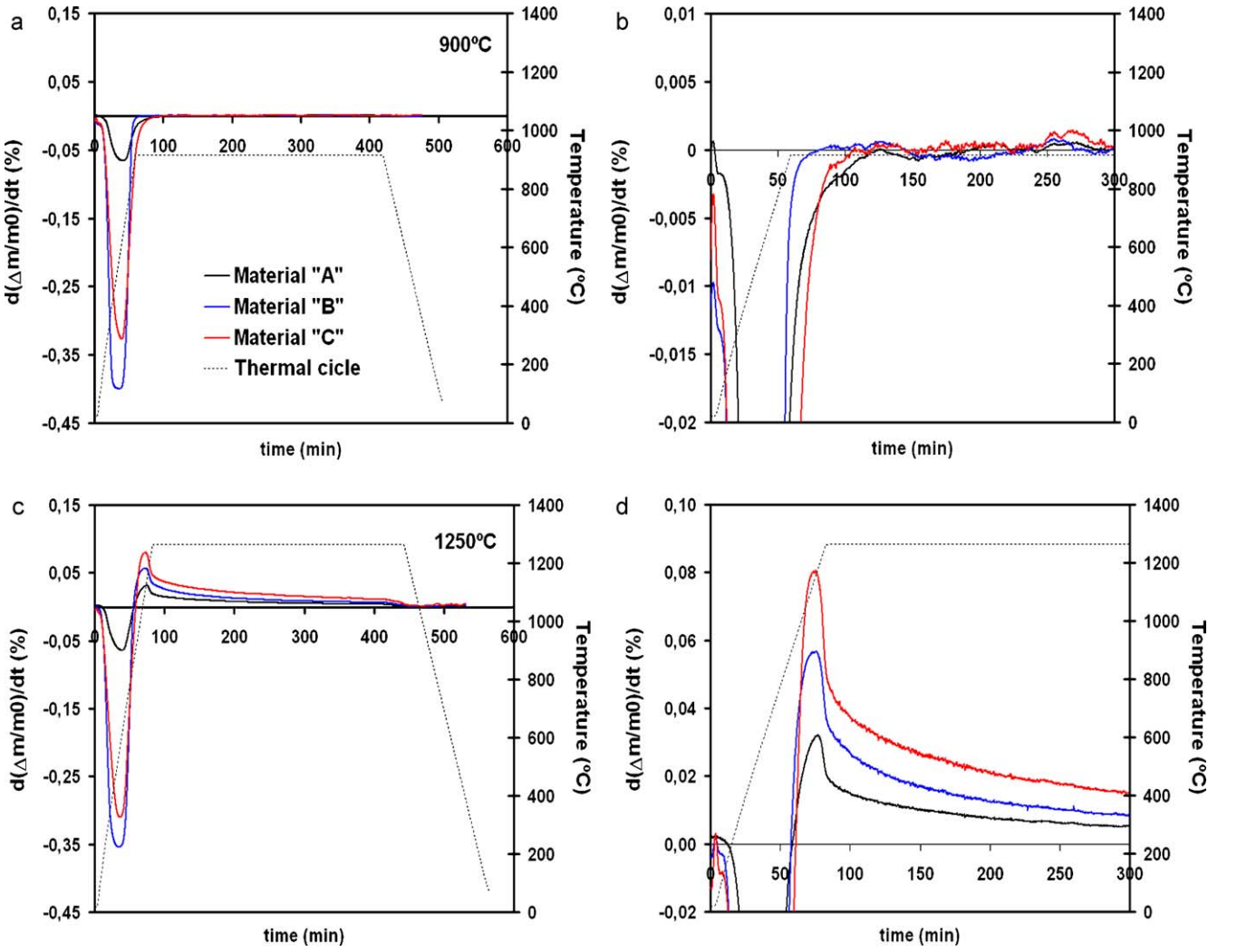

Fig. 5. Derivatives of TGA curves for the tests carried out at: 900 °C (a and b) and 1250 °C (c and d). Images (b) and (d) correspond to a zoom of the region of interest in each case.

the tests carried out at 900 °C, the minimum for material "A" occurs after 132 min after reaching the temperature "plateau" (solid black line Fig. 5b) whereas for material "B" this happens only after 17 min (blue line Fig. 5b). This can be explained by considering that, in materials "A" and "C", Pyro C oxidation occurs at a lower rate due to the small surface area exposed to air between the fiber and the coating. So, the elimination of the Pyro C layer takes longer time than for material "B". Such differences are less important at 1250 °C (Fig. 5d). In this case, the minimums are found at the end of the heating ramp: at 890–985 °C for composites A and B and at 937 °C for material C. This can also be explained by considering that, at 900 °C, the oxidation rate of the Pyro C layers is much higher than that of Tyranno fibers or CVD-SiC coatings. However, at 1250 °C, the oxidation rate of the fiber and the CVD-SiC coating are not negligible. It is, therefore, possible that Pyro C burnout is hindered by the fast growing of silica layers, especially in material "A", since the small gap left between the fiber and the coating can be easily clogged.

After the minimum, mass gain rates present a particular evolution characterized by a sharp maximum at the end of the heating ramp followed by a gradual reduction with time. The magnitude of these maximums also depends on the material composition, being higher for material "C" and decreasing for materials "B" and "A". This is due to the fact that material "C" presents the thinnest CVD SiC coating, that is the highest volume fraction of fibers, which, as will be shown below, are less resistant to oxidation.

A detailed microstructural analysis of TGA samples was not possible due to the small amount of material used in these experiments. The observation of the oxidized layers was carried out on larger specimens tested at the same temperatures in an industrial muffle. The use of these larger samples do not affect the access of oxygen to the PyC layers due to the high porosity of the investigated materials (above 95 vol.%). These tests were extended to longer dwelling times in order to confirm the kinetics observed in TGA experiments. BSE-SEM micrographs corresponding to these samples are included in Fig. 6. These images show also the gaps left between the Tyranno fibers and the CVD-SiC coatings by the Pyro C burnout and the oxide layers growing from the surfaces exposed to air. These oxides generate strong bonds between the fiber and the inner coating surface at the zones

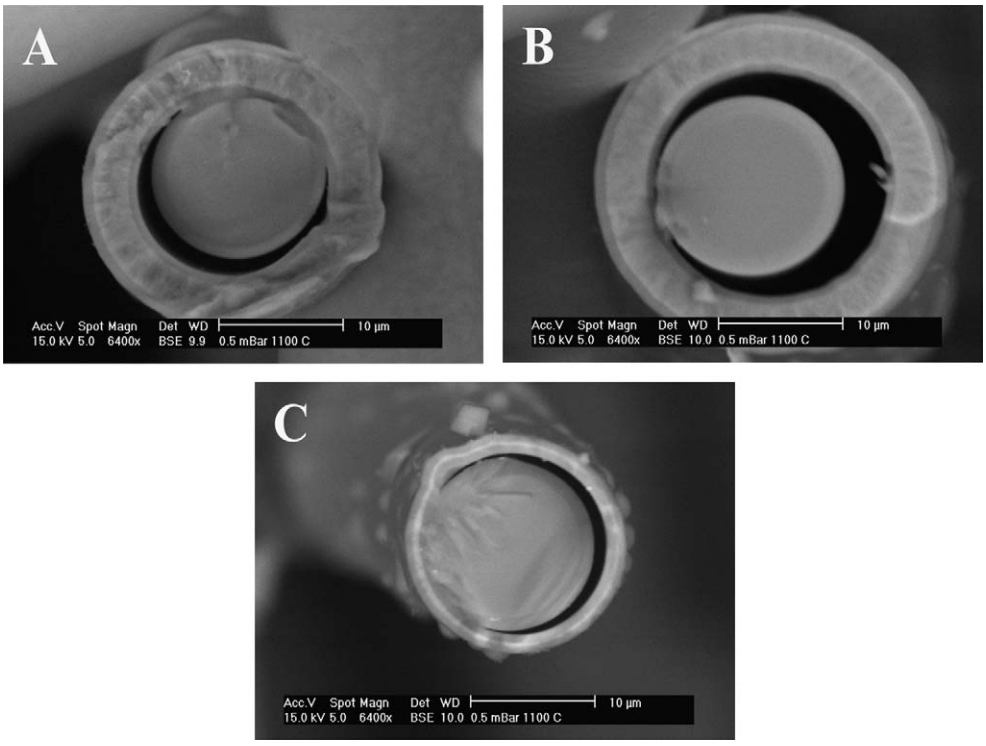

Fig. 6. BSE-SEM images corresponding to composites "A", "B" and "C" oxidized at 1100 °C for 100 h in an industrial muffle.

where they come into contact. The extension of these bonded zones is higher for the composites with thinner Pyro C layers (for instance, in material "C", more than 30% of the fiber surface is bonded to the inner CVD-SiC face). On the other hand, the size of the gap left between fiber and coating decreases with the thickness of the Pyro C layer. A limit situation is found in samples tested at 1100 °C for 2000 h. In these long term experiments, the aforementioned gap appears completely closed in material "A" and still open in material "B" (Fig. 7).

A similar phenomenon has been described for dense SiC/C/SiC composites in which cracks generated at high temperatures in the presence of oxygen are closed by the growth of oxide layers from the crack surfaces.[5,24] This so-called "self healing" behavior protects these dense composites against further Pyro C oxidation and, although it is very unlikely to occur in the composites studied in this work, it emphasizes the strong interaction between both Pyro C and SiC oxidation phenomena in these materials.

Taking these results into account, a first estimation of oxidation kinetics of the Tyranno/Pyro C/CVD-SiC porous composites was carried out from TGA curves by considering the mass gains measured after reaching the parabolic regime (Fig. 8). The data corresponding to the tests carried out at 900 °C were excluded from these calculations, since in this case mass gains do not follow a parabolic trend. The corresponding parabolic rate constants have been calculated from the equation:

$$\left(\frac{\Delta m}{S}\right)^2 = K_m t \quad (1)$$

where $(\Delta m/S)$ is the weight gain per unit surface, K_m is the parabolic rate constant expressed in terms of mass gain, and t, the time. The surface area of the composites ("S") was measured by the BET technique obtaining similar results either for as-deposited or oxidized samples (0.60 m^2/g and 0.62 m^2/g respectively). Although, this suggests that Pyro C burnout does

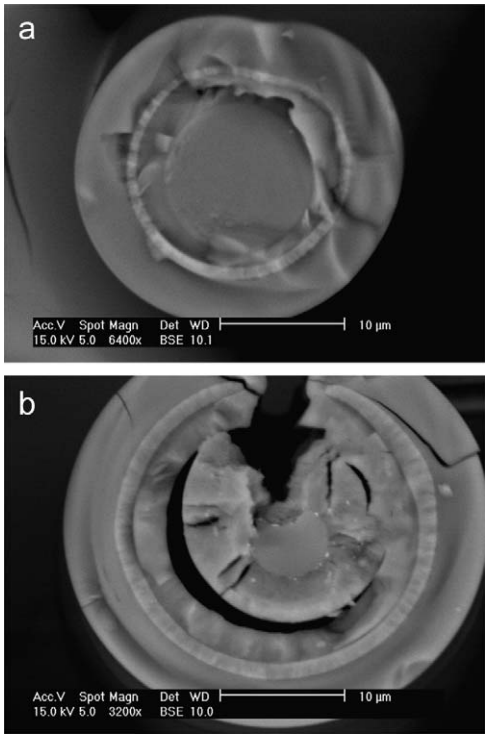

Fig. 7. BSE-SEM images of samples oxidized at 1100 °C for 2000 h showing that the gap between the fiber and the coating is completely closed for material "A" (a) and still open for material "B" (b).

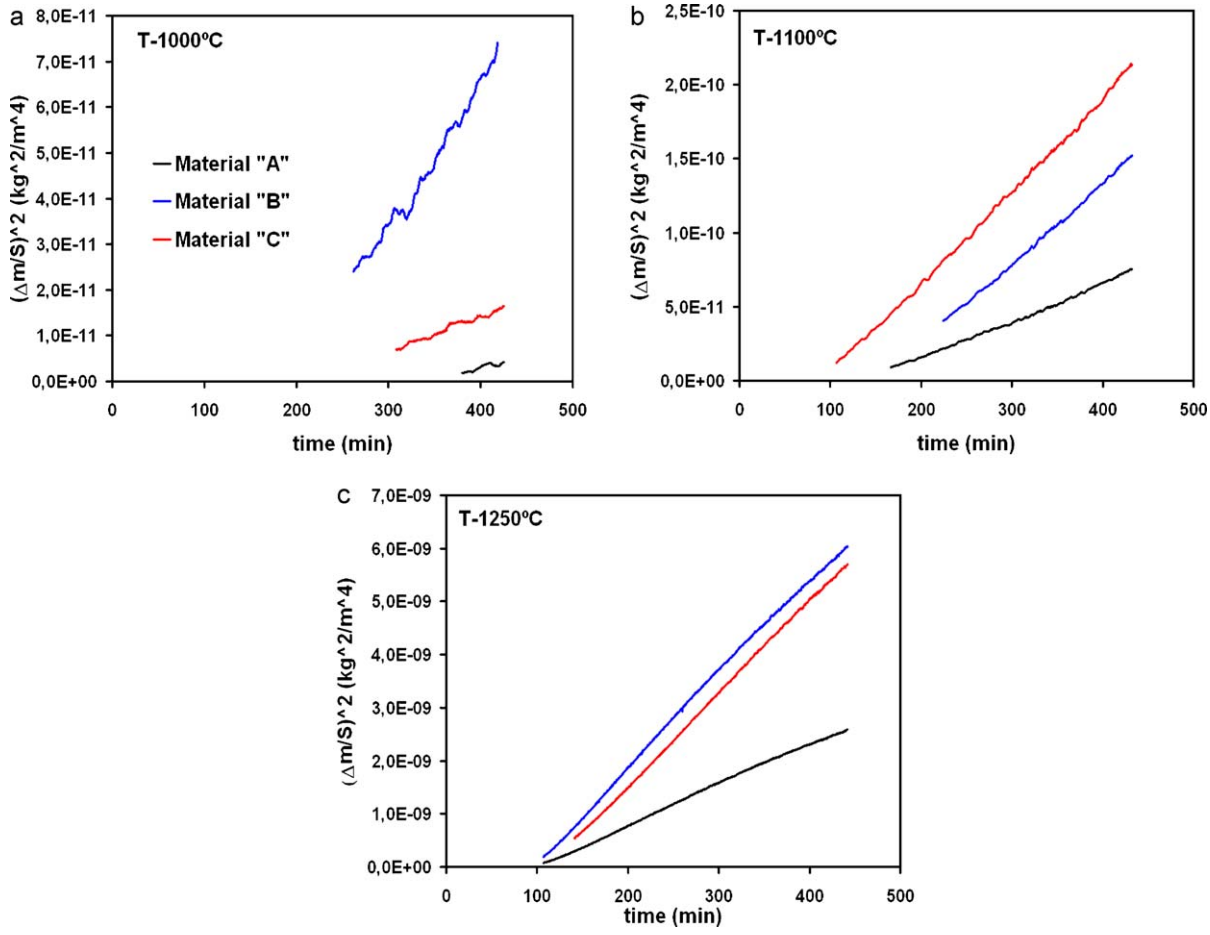

Fig. 8. Specific weight gain squared vs. time for different temperatures: (a) 1000 °C, (b) 1100 °C and (c) 1250 °C.

not produce a significant modification of the surface area of the composites, BET measurements may be misleading because it is possible that the access of the nitrogen (i.e. gas used in these tests) to the gap between the fiber and the CVD coating is limited by the growth of silica layers in this region. The corresponding activation energies (E_{am}) were obtained after confirming that K_m data followed the Arrhenius law (Fig. 9):

$$\ln K_m = \ln K_0 - \frac{E_{am}}{RT} \quad (2)$$

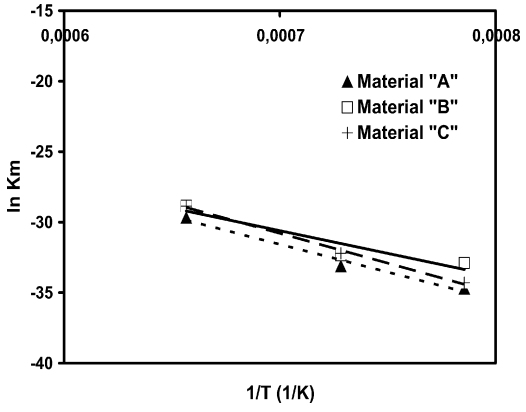

Fig. 9. Arrhenius plot of the parabolic rate constants K_m obtained from TGA experiments.

where K_0 is the so-called pre-exponential constant, E_{am} the apparent activation energy, R the ideal gas constant and T, the temperature in Kelvin degrees.

These activation energies, included in Table 3, are much higher than those reported for single Lox M Tyranno fibers,[4] being close to those reported for CVD-SiC materials[14,20] or SiC single crystals for the (0 0 0 1) face.[19] In TGA oxidation experiments, the Tyranno/Pyro C/CVD-SiC composites are considered as a whole, not taking into account the different oxidation behavior of Lox M Tyranno fibers and CVD-SiC coatings.

Table 3
Activation energies (E_a) and parabolic rate constants (K_m) calculated from TGA experiments.

Reference	T (K)	K_m (kg^2/(m^4 s))	E_{am} (kJ/mol)
A	1273	8.487E−16	327
	1373	4.133E−15	
	1523	1.291E−13	
B	1273	5.160E−15	267
	1373	9.008E−15	
	1523	2.970E−13	
C	1273	1.286E−15	351
	1373	1.031E−14	
	1523	2.922E−13	

In order to analyze the actual oxidation kinetics of each component, the thickness of the different oxide layers have been measured as a function of time from 900 °C to 1250 °C. These graphs also include the data corresponding to the tests carried out at 900 °C since, unlike what has been described for TGA experiments, the thickness of oxides scales produced at this temperature can be measured by FEG-SEM.

These measurements confirmed that the thickness of the different oxide layers follow parabolic laws (Fig. 10b). Similarly to that described for TGA data, the activation energies corresponding to each oxidation process were calculated from the new parabolic rate constants (K_p) after confirming that the Arrhenius law was obeyed in each case (Fig. 11):

$$(\Delta x)^2 = K_p t \tag{3}$$

$$\ln K_p = \ln K'_0 - \frac{E_{ap}}{RT} \tag{4}$$

where Δx is the thickness of the corresponding oxide layer and K'_0 the corresponding pre-exponential coefficient.

The new activation energies (E_{ap}) are considerably lower than those obtained in TGA experiments (compare data of Tables 3 and 4) and agree with those previously reported for both Lox M Tyranno fibers and CVD-SiC coatings in the selected temperature range.[4,14–20] This discrepancy is likely related to the interaction between Pyro C burnout and the formation of the silica layers at the short dwelling times used in TGA test, an effect which tends to underestimate the mass gains and which is probably less important in the experiments carried out in the muffle at longer dwelling times. Nevertheless, TGA experiments are still interesting for qualitative comparisons and as the best possible way of monitoring the Pyro C burnout. Under these considerations and taking into account the activation energies calculated from K_p values, it can be concluded that oxidation kinetics in these SiC/Pyro C/CVD-SiC porous composites is controlled by the inward diffusion of O_2 through the different silicon oxide films.

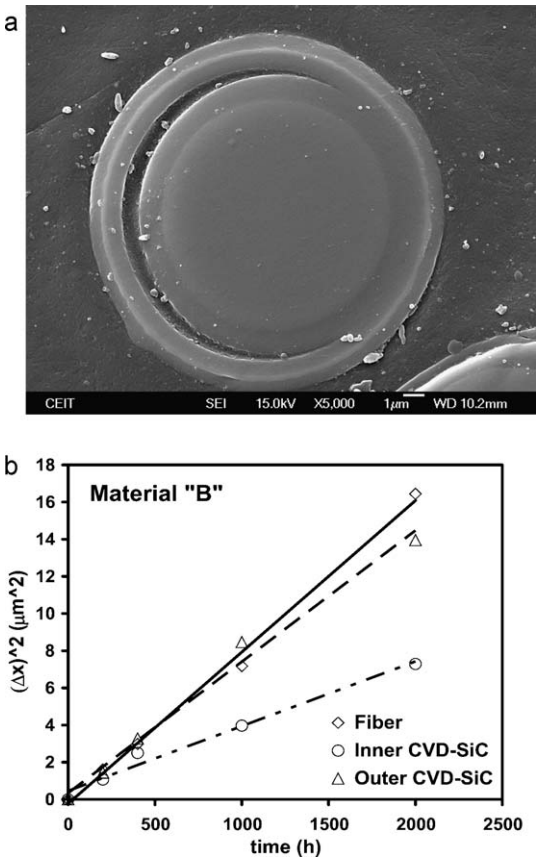

Fig. 10. (a) SEM image of a polished cross section of a specimen mounted in epoxy resin after oxidation at 1100 °C for 100 h and (b) parabolic plot of the oxide scales obtained from these measurements (also at 1100 °C).

These results also confirm that the oxidation resistance of Lox M Tyranno fibers is lower than that of the CVD-SiC coating. The lowest activation energy (i.e. 57 kJ/mol) corresponds to material "B", that with the thickest Pyro C layer. The same tendency is observed in TGA data corroborating that the CVD-SiC coating protects the fiber against oxidation and that this protection is less effective as the size of the gap left after Pyro C burnout

Table 4
Activation energies (E_a) and parabolic rate constants (K_p) calculated from the evolution of oxide layer thickness.

Reference	T (K)	Fiber surface		Inner CVD surface		Outer CVD surface	
		K_p (nm^2/s)	E_{ap} (kJ/mol)	K_p (nm^2/s)	E_{ap} (kJ/mol)	K_p (nm^2/s)	E_{ap} (kJ/mol)
A	1173	1.337	68	0.060	175	0.332	129
	1273	1.889		0.277		0.865	
	1373	3.342		1.431		2.319	
	1523	6.376		3.345		6.824	
B	1173	1.715	57	–	160	0.329	133
	1273	1.509		0.221		1.024	
	1373	3.210		1.224		2.260	
	1523	5.865		2.747		7.891	
C	1173	1.452	62	0.052	225	0.105	154
	1273	1.588		0.208		0.200	
	1373	3.441		1.517		1.090	
	1523	5.684		–		–	

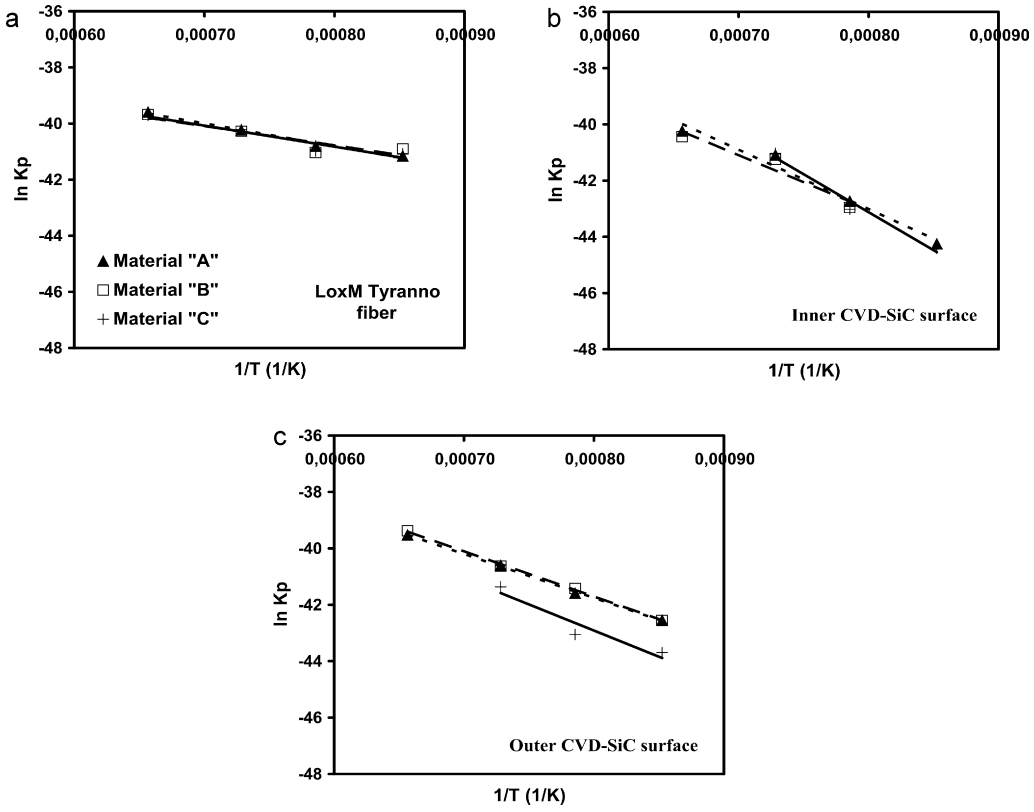

Fig. 11. Arrhenius plots of parabolic rate constants for the oxidation of: (a) Lox M Tyranno fibers, (b) inner surface of CVD-SiC coating and (c) outer surface of CVD-SiC coating.

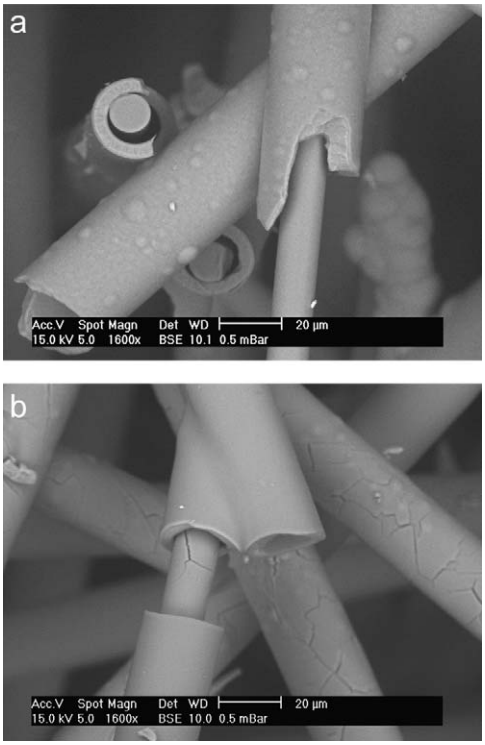

Fig. 12. BSE SEM micrographs corresponding to material "B" tested for 100 h at: (a) 1100 °C and (b) 1250 °C. This latter image shows the presence of cracks at the fiber surface and in the CVD-SiC coating.

increases. This happens in material "B", in which the presence of a wider gap between the fiber and the coating allows an easier access of oxygen to both surfaces.

Another important result is that the CVD-SiC coating exhibits faster oxidation kinetics for the outer than for the inner surface (Table 4). Moreover, it has also been observed that oxidation kinetics accelerate as the coating thickness increases. Thus, materials "A" and "B", both with thick CVD-SiC coatings,

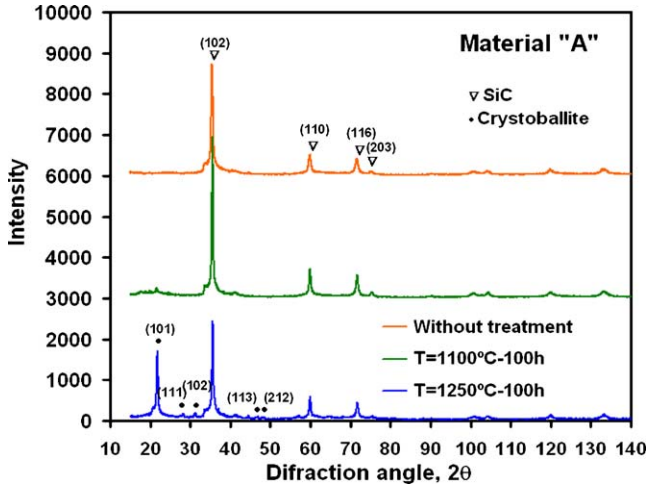

Fig. 13. XRD patterns of material "A" corresponding to: the composite in the initial state (red line) and after oxidation experiments for 100 h at 1100 °C (green line) and 1250 °C (blue line). The latter shows the presence of crystoballite due to the crystallization of the silica layer. (For interpretation of the references to color in this figure legend, the reader is referred to the web version of this article.)

present much thicker outer scales than material "C", with a thinner CVD-SiC coating. These two phenomena are likely related to those described by Ramberg and other authors,[19,29] which confirm that oxidation kinetics in SiC single crystals are anisotropic. TEM studies are in progress in order to analyze the aforementioned differences.

Finally, it has to be pointed out that most of the oxidation tests lead to continuous oxide layers, what is compatible with the observed parabolic kinetics. Nevertheless, the oxide scales of the samples tested at 1250 °C for 100 h presented numerous cracks both at the fiber and the outer CVD-SiC surfaces (Fig. 12). Such cracks are likely due to the strain built-up associated to the high to low cristobalite transformation, since this phase is already present in the oxidized layers (Fig. 13).[4,27]

4. Conclusions

The oxidation of highly porous Tyranno/Pyro C/CVD-SiC composites comprises the Pyro C burnout and the oxidation of the Tyranno fibers and the CVD-SiC coatings. Within the selected temperature range (from 900 °C to 1250 °C), it has been confirmed that the phenomena leading to mass gain (i.e. silica formation from the oxidation of the fibers and the coatings) exhibit parabolic kinetics. The activation energies obtained from the evolution of the thickness of the silica layers with temperature agree with those related to the inward diffusion of O_2 through the silica scale. However, the onset of the silica cracking observed in the tests carried out at 1250 °C suggest a change of tendency at higher temperatures.

TGA experiments confirm that Pyro C burnout is faster for the composites with thicker Pyro C layers, although, at 1250 °C, such difference is less evident. This could be due to the interaction between Pyro C burnout and the formation of silica layers which is stronger as the temperature increases. Finally, it has been confirmed that the oxidation resistance of CVD-SiC coatings is higher than that of the Lox M Tyranno fibers, although it is not homogeneous. Thus, the outer surface of the coating presents a thicker silica layer than that found at the inner surface. Moreover, the oxidation resistance of the coating is observed to decrease as its thickness increases. A possible explanation for these phenomena could be related to anisotropic effects.

Acknowledgements

The authors thank the Departamento de Industria, Comercio y Turismo del Gobierno Vasco and CDTI for the financial support given to this work.

References

1. Chermant JL. *Les Céramiques Thermomécaniques*. Paris: Presses du CNRS; 1989.
2. Viricelle JP, Goursat P, Bahloul-Hourlier D. Oxidation behaviour of a multilayered ceramic-matrix composite $(SiC)_f/C/(SiBC)_m$. *Compos Sci Technol* 2001;**61**:607–14.
3. Naslain R. Design, preparation and properties of non-oxide CMCs for application in engines and nuclear reactors: an overview. *Compos Sci Technol* 2004;**64**:155–70.
4. Chollon G. Oxidation behaviour of ceramic fibers from the Si–C–N–O system and related sub-systems. *J Eur Ceram Soc* 2000;**20**:1959–74.
5. Naslain RR. Chemical reactivity in the processing and the interactions with the environment of ceramic matrix composites. *Solid State Ionics* 1997;**101–103**:959–73.
6. Laffon C, Flank AM, Lagarde P, Laridjani M, Hagege R, et al. Study of Nicalon-based ceramic fibres and powders by EXAFS spectrometry, X-ray diffractometry and some additional methods. *J Mater Sci* 1989;**24**(4):1503–12.
7. Shimoo T, Kakehi Y, Kakimoto K, Okamura K. Oxidation kinetics of amorphous Si–Ti–C–O fibers. *J Jpn Inst Metals* 1992;**56**(2):175–83.
8. Shimoo T, Chen H, Okamura K. High-temperature stability of nicalon under Ar or O_2 atmosphere. *J Mater Sci* 1994;**29**:456–63.
9. Mah T, Lecht N, McCullum DE, Hoenigman JR, Kim HM, Katz AP, Lipsitt HA. Thermal stability of SiC fibers nicalon. *J Mater Sci* 1984;**19**:1191–201.
10. Clark TJ, Prack ER, Haider MI, Sawyer LC. Oxidation of SiC ceramic fiber. *Ceram Eng Sci Proc* 1987;**8**(7–8):717–31.
11. Johnson SM, Brittain RD, Lamoreaux RH, Rowcliffe DJ. Degradation mechanisms of silicon carbide fibers. *J Am Ceram Soc* 1988;**71**:C132–5.
12. Pailler R, Chollon G, Hannache H, Naslain R, Pillot JP, Dunogues J, Birot M, Influence of different curing processes on the thermal stability of ceramic fibers derived from organosilicon precursors, Adv Stuct Fiber Comp. In: Vincenzini P, editor. Advances in science and technology, Faenza: Techna Publishers; 1995. p. 69–76.
13. Bodet R, Jia N, Tressler RE. Microstructural instability and the resultant strength of Si–C–O nicalon and Si–N–C–O HPZ fibers. *J Eur Ceram Soc* 1996;**16**:653–64.
14. Narushima T, Goto T, Hirai T. High temperature passive oxidation of chemically vapor deposited silicon carbide. *J Am Ceram Soc* 1989;**72**(8):1386–90.
15. Costello JA, Tressler RE. Oxidation kinetics of silicon carbide crystals and ceramics: I, In dry oxygen. *J Am Ceram Soc* 1986;**69**(9):674–81.
16. Luthra KL. Some new perspectives on oxidation of silicon carbide and silicon nitride. *J Am Ceram Soc* 1991;**74**(5):1095–103.
17. Jacobson NS. Corrosion of silicon-based ceramics in combustion environments. *J Am Ceram Soc* 1993;**76**(1):3–28.
18. Spear KE, Tressler RE, Zheng Z, Du H. Oxidation of silicon carbide single-crystal and CVD silicon nitride. In: Tressler RE, McNallan M, editors. *Ceramic transactions*, vol. 10. Westerville, OH: The American Ceramic Society; 1990. p. 1–18.
19. Ramberg CE, Cruciani G, Spear KE, Tressler RE. Passive-oxidation kinetics of high-purity silicon carbide from 800 °C to 1100 °C. *J Am Ceram Soc* 1986;**79**(11):2897–911.
20. Sucov EW. Diffusion of oxygen in vitreous silica. *J Am Ceram Soc* 1963;**46**(1):14–20.
21. Williams EL. Diffusion of oxygen in fused silica. *J Am Ceram Soc* 1965;**48**(4):190–4.
22. Muehlenbachs K, Schaeffer HA. Oxygen diffusion in vitreous silica. *Can Miner* 1977:179–84.
23. Naslain R, Guette A, Rebillat F, Le Gallet S, Lamouroux F, Filipuzzi L, Louchet C. Oxidation mechanisms and kinetics of SiC-matrix composites and their constituents. *J Mater Sci* 2004;**39**:7303–16.
24. Filipuzzi L, Camus G, Naslain R, Thebault J. Oxidation mechanisms and kinetics of 1D-SiC/C/SiC composite materials: I, An experimental approach. *J Am Ceram Soc* 2005;**77**(2):459–66.
25. Ube. Tyranno fiber catalogue. http://www.upilex.jp/catalog/pdf/tyranno_fiber_e.pdf.
26. Oishi T, Tanaka Y, Miyamoto N, Suzuki M, Sato M, United States patent application 2008/0226885/A1; September 18, 2008.
27. Naplocha K, Janus A, Kaczmar JW, Samsonowicz Z. Technology and mechanical properties of ceramic preforms for composite materials. *J Mater Process Tech* 2000;**106**(1–3):119–22.
28. Song JI, Yang YC, Han KS. Squeeze-casting conditions of Al/Al_2O_3 metal matrix composites with variations of the preform drying process. *J Mater Sci* 1996;**31**(10):2615–21.
29. Radmilovic V, Dahmen U, Gao D, Stoldt CR, Carraro C, Maboudian R, Formation of b111N fiber texture in β-SiC films deposited on Si(1 0 0) substrates. 2007;16:74–80.